Influence of Particle Size, Air Flow, and Inhaler Device on the Dispersion of Mannitol Powders as Aerosols

Nora Y. K. Chew[1] and Hak-Kim Chan[1,2]

Received January 4, 1999; accepted April 12, 1999

Purpose. To study the effect of particle size, air flow and inhaler type on the dispersion of spray dried mannitol powders into aerosols.
Methods. Mannitol powders were prepared by spray drying. The solid state properties of the powders were determined by laser diffraction, X-ray powder diffraction, scanning electron microscopy, freeze fracture, Karl Fischer titration and gas pycnometry. The powders were dispersed using Rotahaler® and Dinkihaler®, connected to a multistage liquid impinger at different air flows.
Results. Three crystalline mannitol powders with primary particle size (MMD) 2.7, 5.0, 7.3 μm and a similar polydispersity were obtained. The particles were spherical with a density of 1.5 g/cm^3 and a moisture content of 0.4 wt.%. At an air flow of 30 L/min all the powders were poorly dispersed by both inhalers. With the Rotahaler® increasing the flow (60–120 L/min) increased the fine particle fraction (FPF) in the aerosols for the 2.7 μm powder, and decreased the FPF for the 7.3 μm powder; whereas the FPF for 5.0 μm powder was unaffected. With the Dinkihaler®, all the powders were near complete dispersion at ≥60 L/min.
Conclusions. The FPF in the mannitol powder aerosols was determined by an interplay of the particle size, air flow and inhaler design.

KEY WORDS: mannitol; dry powder inhaler; powder aerosol; particle size; air flow; inhalation.

INTRODUCTION

Mannitol, a hexahydric alcohol ($C_6H_{14}O_6$, molecular weight 182), is primarily used as a pharmaceutical excipient. Its potential use as a carrier for aerosol delivery of proteins has been also reported (1,2). More recently, we have developed spray dried mannitol powder as an aerosol preparation for bronchial provocation testing in asthmatics (3) and for the enhancement of mucociliary clearance in both normal and asthmatic subjects (4).

Aerosol drug delivery by dry powder inhalers has drawn considerable attention during recent years. Various important factors which affect dry powder aerosol delivery have been reported. These include: humidity (5), air flow (6,7), effect of carrier (8), particle surface nature (9) and inhaler resistance (10). Although the influence of particle size on the clinical outcome of aerosols was extensively reported (11,12), very little attention has focused on the effect of primary particle size on the in vitro aerosol generation by dry powder inhalers (2,13). This is partly due to the constraint of using commercial inhalers, where the particle size of the powders is fixed.

[1] Department of Pharmacy, University of Sydney, NSW 2006, Australia.
[2] To whom correspondence should be addressed. (e-mail: kimc@pharm.usyd.edu.au)

The purpose of the present work is to study the effect of particle size and air flow on the aerosolization of spray dried mannitol powders using two different inhalers, and to gain a fundamemal understanding on the interplay of these physical factors on aerosol generation.

MATERIALS AND METHODS

Preparation of Mannitol Powders

Spray dried mannitol powders of three different particle sizes were obtained using a Büchi 191 Mini Spray Dryer (Flawil, Switzerland). Table 1 provides a summary of the spray drying conditions. The feed solution contained only mannitol dissolved in deionized water. The running time was approximately 8 hr per batch. To have sufficient amounts for dispersion experiments, several batches of powders with the same particle size were collected and mixed together (Turbula mixer, Basel, Switzerland). The powders were stored over silica gel until use.

Solid State Characterization

Scanning Electron Microscopy (SEM)

Powder samples were mounted onto metal sample plates and coated with gold. The samples were then examined under a Joel JSM 6000F scanning electron microscope (Tokyo, Japan) operating at 4kV.

X-Ray Powder Diffraction (XRD)

Powder crystallinity was assessed by XRD. Equal amounts of the mannitol powder and an internal reference standard material (silicon powder, 640b, National Bureau of Standards, USA) were thoroughly mixed and then packed on a glass sample plate under the same storage humidity. The samples were measured on a Siemens D5000 X-ray powder diffractometer (Hamburg, Germany) using CuK_α radiation, 40 kV and 30 mA, angular increment of 0.05°/sec and an increment count time of 2.0 sec.

Moisture Content Determination

Water content of the mannitol powders (10 mg) was determined in triplicate by Karl Fischer titration (737 KF Coulometer, Metrohm, Herisau, Switzerland).

Density Determination

The true density of the spray dried powders was determined by gas displacement pycnometry (model 1350, Micromeritics Instruments, Norcross, GA) and buoyancy method (14). Powder samples (1–2 mg) were placed in a density gradient liquid (comprising bromoform and 1-hexanol) and centrifuged (Jouan CT422, Saint Herblain Cedex, France) at 3500 rpm and 5°C for 30 min. The particle density was equal to the liquid density when the particles remained stationary in the liquid after centrifugation.

Freeze Fracture of Spray Dried Powders

Freeze fracture was carried out to examine the interior of the individual particles. A frozen aliquot of a powder suspension

0724-8741/99/0700-1098$16.00/0

Table 1. Spraying Conditions for Mannitol Powders [Mannitol Raw Material (AR Grade) was Supplied from Sigma (St. Louis, MO) and Mallinckrodt (Paris, KY)]

Feed concentration (mg/ml)	Inlet Temperature (°C)	Outlet Temperature (°C)	Feed rate (ml/min)	Aspiration (m^3hr^{-1})	Compressed air pressure (kPa)
10	110	75	1.4	57.6	750–800
100	130	85	1.4	57.6	400–500
100	140	88	4.0	57.6	350–400

in sunflower oil (Florafoods, Marrickville, Australia) was fractured in a freeze-etch unit (BAF 300, Balzers, Liechtenstein) at −100°C. A replica of the fracture surface was made by shadowing with platinum/carbon (approx. 150 nm thick) and a carbon backing layer (approx. 200 nm thick) was then added. After cleaning and mounting, the replica was viewed under a Philips 400 transmission electron microscope (Eindhoven, The Netherlands) operating at 100 kV.

Particle Sizing of Spray Dried Powders

Particle size distribution of the powders was measured in suspensions using a Mastersizer S Laser Diffractometer (Malvern, Worcs, UK) as described previously (2). Chloroform was used as a dispersion medium. Particle size analysis was based on the refractive index (RI) of mannitol (1.330), $RI_{imaginary}$ of mannitol (0.100) and RI of chloroform (1.444). The size distribution was expressed by the volume median diameter (VMD) and span. VMD is related to the mass median diameter (MMD) by the density of the particles (assuming a size-independent density for the particles). Span is a measure of the width of the size distribution. Span = [D(v, 90) − D(v, 10)]/D(v, 50), where D(v, 90), D(v, 10) and D(v, 50) are the equivalent volume diameters at 90, 10 and 50% cumulative volume, respectively.

Aerosol Characterisation—Effect of Flow and Particle Size

Studies were conducted in an airtight perspex glove box (dimensions 45 × 75 × 80 cm), housing the impinger and other accessories. The humidity inside the box was regulated via feedback from a temperature and humidity probe (HMP 35, Vaisala, Helsinki, Finland) to a controller that activated or deactivated a humidifier (Ventalaire nebuliser, Allersearch, Sydney, Australia) and dehumidifier (silica gel-filled column, 82 cm in length, 6 cm in diameter connected to an air pump) according to the required humidity. To minimize potential changes in the powders due to crystallization (1,15), the relative humidity (RH) of the perspex glove box was maintained at 23% (range 15–35%). Prior to dispersion, the powders were stored at the same humidity in a desiccator over saturated potassium acetate solution for a minimum of 12 hr.

The dispersion behavior (the breaking up of agglomerates to regenerate the primary particles) of the spray dried powders was assessed by a Rotahaler® (Allen & Hanburys) and a Dinkihaler® (Fisons) coupled to a 4-stage (plus filter) liquid impinger (Copley, Nottingham, UK) as described previously (2). Both inhalers are capsule devices and have a similarly low air flow resistance of 0.03 (Rotahaler®) and 0.04 (Dinkihaler®) $cmH_2O^{1/2}$/L/min, but differ in their mode of powder emptying and dispersion (see Discussion).

Approximately 20 mg of powder was weighed into a gelatin capsule (size 3, Park Davis, Australia; pre-equilibrated at 44%RH) at room conditions (20 ± 1°C, 57 ± 5%RH). Plastic capsules of similar dimensions were used for the runs at 90 and 120 L/min using the Dinkihaler® due to shattering of the gelatin capsules. Immediately after filling, the capsule was loaded into the inhaler and the powder was dispersed into the running impinger. A total of 10 capsules were dispersed. Mannitol was assayed by vapour pressure osmometry using a Knauer differential vapor pressure osmometer (model no. 11.00, Berlin, Germany) at 37°C with deionised water as the reference. A calibration curve was constructed using standard solutions of mannitol: Instrument signal (mV)= 16.15*concentration(mg/ml)[n = 16, R^2 = 0.998].

Fine particle fraction (FPF) is defined as the mass fraction of particles smaller than a certain size in the aerosol. The sizes chosen were ≤ 4.4, 6.8, 5.5 and 4.8 μm at 30, 60, 90 and 120 L/min, respectively, due to the flow-dependence of the cutoff size of the impinger stages which are inversely proportional to the square root of the air flow (16). Numerically, FPF is the percentage of powder collected from stage 4 and filter at 30 L/min and from stages 3, 4 and filter at 60, 90 and 120 L/min. FPF is referenced against the recovery (i.e. total dose = emitted dose + device and capsule retention), and is expressed as the means of triplicate runs. Student t-test was performed with probability values of less than 0.05 considered as statistically significant.

RESULTS

Solid State Characterization

The three spray dried mannitol powders had unimodal particle size distribution, with mass median diameters (MMD) of 2.7, 5.0 and 7.3 μm (corresponding polydispersity as expressed by the span were 1.9, 1.7, 1.9). The powders consisted of spherical particles with surfaces resembling a composite of elongated mannitol crystals (Fig. 1a). The powders had a similar degree of crystallinity which was lower than that of the raw material (Fig. 2), a low water content of 0.4 wt.% and a similar density, range 1.45–1.53 g/cm^3, which agrees with the literature values of 1.48–1.52 g/cm^3 (17,18). The results were similar in both the pycnometry and the buoyancy method, suggesting that these particles were not hollow. This was supported by the freeze fracture results (Fig. 1b) that revealed the interior features of the particles. Hence, the mass median aerodynamic diameters (MMAD) of mannitol powders could be calculated from the product of MMD and the square root of density (19), using a density of 1.5 g/cm^3.

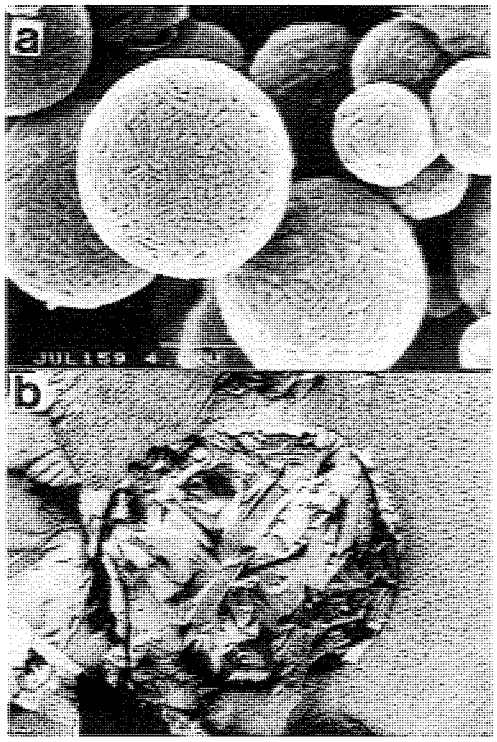

Fig. 1. (a) Scanning electron micrograph of spray dried mannitol powder, MMD 2.7 μm; scale bar 1 μm (similar spherical morphology was observed for 5.0 and 7.3 μm powders). (b) Transmission electron micrograph of freeze fractured mannitol particle (magnification 3550x).

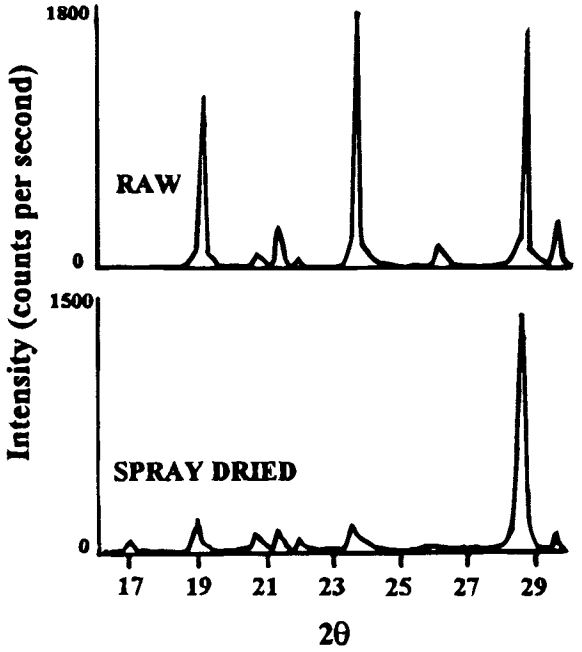

Fig. 2. X-ray diffraction patterns of raw material and spray dried mannitol powders, MMD 2.7 μm (similar pattern occurred for 5.0 and 7.3 μm powders; the diffraction peak at 2θ angle of 28.4° belongs to the internal standard silicon powder).

Aerosol Characterization

Rotahaler®

Using the Rotahaler®, the fine particle fraction (FPF) was increased proportionately with the air flow for the 2.7 μm (MMD) powder (Fig. 3a). The effect was not seen for the 5.0 μm powder dispersed at ≥60 L/min. A further increase in the primary particle size to 7.3 μm actually reversed the trend of flow-dependence at ≥60 L/min, i.e., FPF decreased with higher flows.

Figure 4 compares the particle size distribution curves of the original powders (determined by laser diffraction) to that of the aerosols generated by the Rotahaler® (determined by the multiple stage liquid impinger). The aerosol curves are situated above the original powder curve, indicating that the powders were not sufficiently dispersed by the inhaler to recover the primary particle size distribution. For the 2.7 μm powder the aerosol curve was shifted toward the original powder curve as the air flow was increased (Fig. 4a). However, even at the highest flow of 120 L/min, the primary particle size distribution was not recovered. In comparison, when the 5.0 μm powder

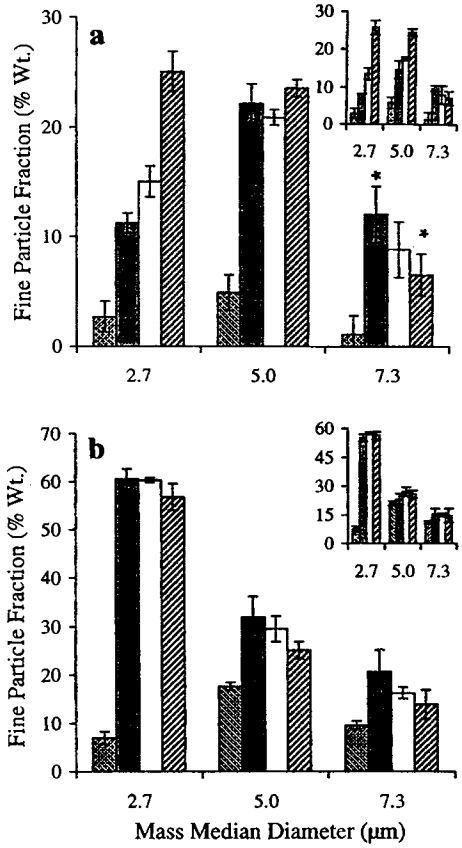

Fig. 3. (a) Effect of particle size and air flow (30 L/min ▩, 60 L/min ■, 90 L/min □, 120 L/min ▨) on the dispersion of spray dried mannitol powders using Rotahaler® (*$p < 0.05$ between 60 and 120 L/min only). The inset shows the interpolated FPF based on particles ≤ 5 μm (see Text). (b) Effect of particle size and air flow (30 L/min ▩, 60 L/min ■, 90 L/min □, 120 L/min ▨) on the dispersion of spray dried mannitol powders using Dinkihaler®. The inset shows the interpolated FPF based on particles ≤ 5 μm (see Text).

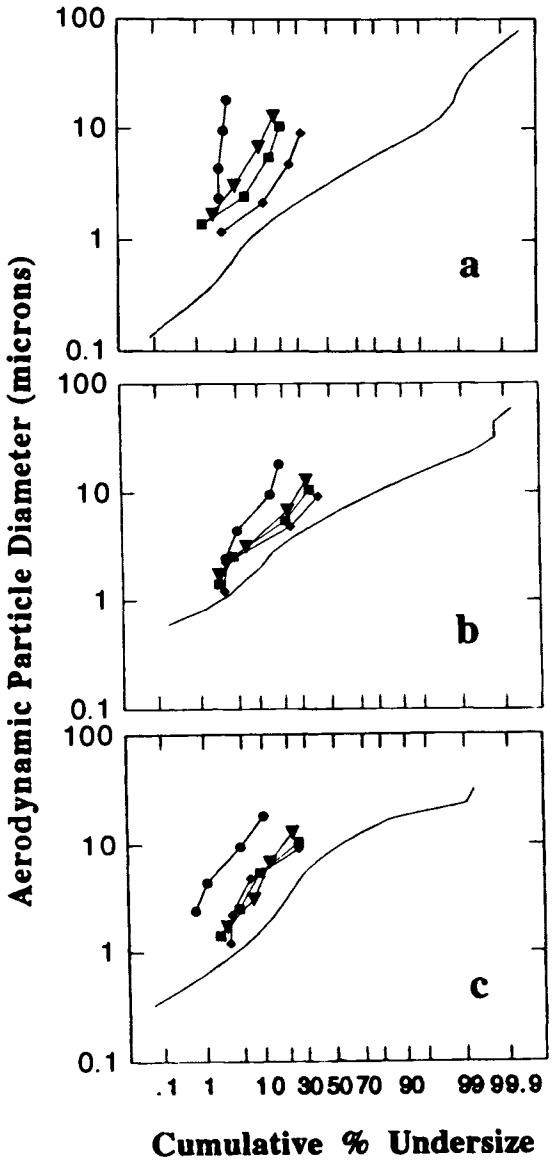

Fig. 4. Comparison of the particle size distribution of spray dried mannitol powders (a. 2.7 μm, b. 5.0 μm, c. 7.3 μm) before (solid line) and after dispersion using Rotahaler® at different air flow (30 L/min —●—, 60 L/min —▼—, 90 L/min —■—, 120 L/min —◆—).

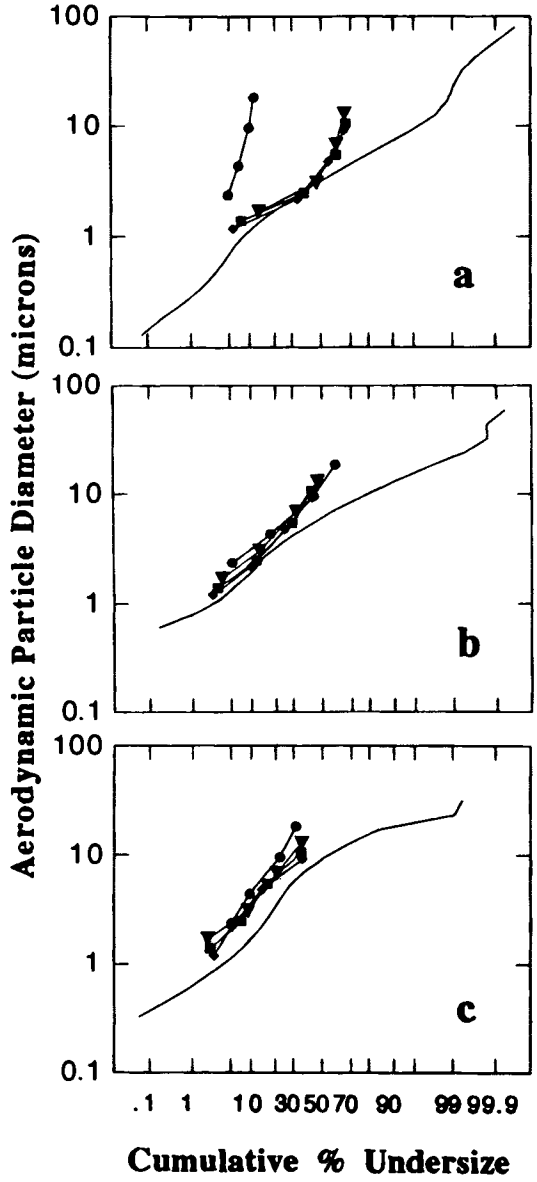

Fig. 5. Comparison of particle size distribution of spray dried mannitol powder (a. 2.7 μm, b. 5.0 μm, c. 7.3 μm) before (solid line) and after dispersion using Dinkihaler® at different air flow (30 L/min —●—, 60 L/min —▼—, 90 L/min —■—, 120 L/min —◆—).

was dispersed, the aerosol curves were shifted closer to each other and to the powder curve (Fig. 4b). Increasing the primary particle size further to 7.3 μm did not shift the aerosol curves closer to the powder curve (Fig. 4c).

Dinkihaler®

Using the Dinkihaler® the 2.7 μm powder was almost completely dispersed at air flows ≥60 L/min, as shown in the size distribution curves of the aerosols (Fig. 5a). Consequently, there was no flow dependence on the FPF and the FPF was much higher than that obtained by the Rotahaler® (Fig. 3b). Similarly, the 5.0 μm powder shows near complete dispersion and higher FPF at flows ≥60 L/min. Even at the low flow of 30 L/min, the dispersion efficiency was still reasonably high (Figs. 5b & 3b). For the 7.3 μm powder, the aerosol curves were situated slightly above the powder curve with increasing flow (Fig. 5c). There was a slight decrease in FPF with increase in air flow (Fig. 3b) but it was not statistically significant ($p > 0.1$).

The dispersion results have been expressed as FPF corresponding to different cutoff diameters at the different air flows. While the use of FPF (in Figs. 3 a & b) simplifies the comparison, it suffers from the limitation of describing only a single particle size. For this reason, the entire particle size distributions of the aerosols at different flows are provided (Figs. 4 & 5). The FPF can then be standardized at the same size by interpolation to the cumulative percent undersize at e.g., 5 μm (Figs. 3 a & b insets). The results were in good qualitative agreement with the general trends of FPF discussed above.

Powder Emptying from Inhalers

The amounts of powder emptied from both inhalers were similar at air flows ≥60 L/min [Rotahaler®: 75 (±7) wt.%, range 66–88; Dinkihaler®: 82 (±4) wt.%, range 74–87; the rest was retained in the capsules and devices]. However, at 30 L/min, only 31 wt.% of the 7 μm powder and 46 wt.% of the 5 and 2.7 μm powders were emitted from the Rotahaler®, indicating insufficient powder emptying from the device at the low flow. In comparison, at 30 L/min the emptying of the 5 and 7 μm powders from the Dinkihaler® was unaffected (74 ± 2 wt.%) but that of the 2.7 μm powder was greatly reduced to 28 wt.%. Powder agglomerates were found retained inside the capsules. By enlargement of the holes at the capsule ends to the maximum size of 5 mm, the emptying of the 2.7 μm powder was increased to 60 (±1) wt.% but the FPF was only increased to 19 (±2) wt.%.

DISCUSSION

This study demonstrated that the dispersion behavior of mannitol powders depends on an interplay between the primary particle size, air flow and inhaler design. In general, for small particles, increasing the air flow and the inhaler dispersion efficiency increased the fine particles in the aerosol cloud. For large particles, the dependence of dispersion on air flow and inhaler was weaker, and might even be slightly reversed at higher air flows due to impaction loss of particles at the throat of the impinger. The amount of fine particles in the aerosols thus depends on exactly what inhaler, air flow and powder were used.

The powders had consisted of solid (non-porous) particles with the same true density. The unimodal size distributions with a similar polydispersity, but differed only in the median particle size for the powders made it feasible to use the median particle size for comparing the dispersion behavior. Different polydispersities would have affected the contact areas (hence cohesion) between particles (20) and complicated the comparison.

The effect of the particle size can be explained by the particle cohesiveness due to the universal van der Waals force of attraction, electrostatic charge interaction and capillary force. The van der Waals force (F_{vdw}) between two identical spheres is given by (21):

$$F_{vdw} = A.R/12H^2 \quad (1)$$

where R is the radius of the particles, A the van der Waals constant, H the separation distance between the particles. When the separation distance vanishes (H approaches zero), the cohesion force, F_c, becomes (21):

$$F_c = 2\pi\sigma R \quad (2)$$

where σ is the surface tension of the particles or of any adsorbed film on the particles. Because of the low moisture content of the powders and the low relative humidity at which the dispersion was carried out, capillary force from adsorbed moisture is likely to be insignificant. The presence and/or significance of electrostatic interaction was undetermined in this study.

Based on both Eqs. (1) & (2), the force of attraction per unit mass of particles is inversely proportional to the square of the particle size. Thus finer particles would be more cohesive and difficult to disperse. This is consistent with the Rotahaler® results at low flows. This was also evidenced by the agglomerates retained in the capsule when the 2.7 μm powder was dispersed by the Dinkihaler® at the low flow (30 L/min) and by the slow increase in the FPF even when the emptying of the powder was increased.

The flow-dependence of FPF in the Rotahaler® is commonly seen with commercial inhalers (22) and can be attributed to the powder cohesiveness as just described and/or the inadequate dispersion efficiency of the inhaler. The powder in the Rotahaler® is dispersed simply by the air flowing through a grid in the mouthpiece whereas in the Dinkihaler® the powder is emptied and dispersed from a small hole at each end of the capsule spinning at ≥1200 rpm (measured by a stroboscope, IEC, Melbourne, Australia), and is further dispersed through the mouthpiece by the air entrained from the two air inlets of the inhaler (Fig. 6). The action of air flow on the powders in Dinkihaler® is thus different from, and perhaps more turbulent than that in the Rotahaler®. The Dinkihaler® is apparently more efficient as more complete dispersion of the 2.7 μm powder is achieved at the same air flows.

The effect of air flow on powder dispersion has been explained by Fuchs in a simplistic manner (20). An agglomerate located in a velocity gradient (Φ) is subjected to a difference of flow velocity (2RΦ) at two points separated by a distance of 2R, where R is the particle radius. A detachment force F_d results, tending to separate two particles in contact:

$$F_d \approx 12\pi\eta R^2\Phi \quad (3)$$

where η is the air viscosity. Thus, particle separation would be more difficult with a low velocity gradient and small particles. For detachment of particles less than 10 μm, the gravitational force becomes negligible as compared to aerodynamic force due to air flows (23). In turbulent flows it is believed that particles detach from a surface by a rolling motion rather than lifting and the critical shear velocity required to detach the particles is, besides other adhesion parameters, proportional to 1/(particle diameter)^n, where n depends on the theoretical model employed (24). Thus, small particles require a higher shear velocity for detachment which appears to be consistent with our observations with the 2.7 μm powder using higher air flows or using a higher efficiency device. Unfortunately, the actual

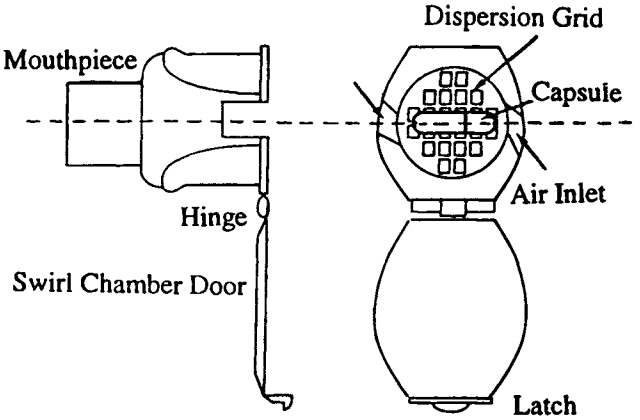

Fig. 6. The Dinkihaler®. The inhaler consists of a small cylindrical swirl chamber with two tangential air inlets. To the rear of the chamber is a door which allows loading and unloading of capsules.

shear velocities at different air flows were unavailable for further comparison.

Larger particles are less cohesive (lower specific surface area and van der Waals force per unit mass of particles) and because of a greater detachment force (Eq. 3), these particles are expected to separate easier, but there will be lesser fine particles available. This was found for the 7.3 μm powder dispersed by both inhalers (Fig. 3 a&b). In addition, larger particles are more likely to deposit at the throat of the impinger by inertial impaction (proportional to the air flow and the square of particle size). This was confirmed by the increasing amount of the 7.3 μm powder collected at the throat and stage 1 of the impinger with increasing air flow using the Rotahaler® (44.1, 56.1 and 62.3% at 60, 90 and 120 L/min, respectively) [With the Dinkihaler® the values leveled at 50 ± 2% once the flow reached 60 L/min]. The maximum FPF is thus the result of a balance of the particle cohesion and inhaler efficiency against the available fine particles at a specific air flow. This was achieved in the 5.0 μm powder using the Rotahaler®, and in the 2.7 μm powder using the Dinkihaler®, at ≥60 L/min. However, the FPF was much higher with the Dinkihaler® than with the Rotahaler®, due to the difference in the inhaler design and the dispersion mechanism as discussed earlier. The independence of FPF on air flow for the 5.0 μm powder in the Rotahaler® indicates that the impaction loss at the higher air flows is balanced by the availability of more fine particles. The low flow (30 L/min) is insufficient to disperse the powder by both inhalers, as shown in all three powders.

The dependence of dry powder aerosol performance on air flow has been previously reported (22 & references therein). An implication from the present data is that the flow dependence in the Rotahaler® can be diminished by increasing the primary particle size of a powder (without undue impaction loss). However, when formulating dry powders for inhalation, one would generally tend to use smaller primary particles to enhance the chance of aerosol penetration into the lung. Therefore, the use of larger particles may not be obvious to the formulator as a feasible approach to reduce the flow dependency while still maintaining sufficiently high fine particle mass in the aerosol. Another implication is that given a dry powder formulation, the amount of fine particles in the aerosols can be improved by switching to a higher efficiency inhaler. Thus, all three parameters: the inhaler, the air flow and the particle size have to be simultaneously taken into account when optimizing the aerosol performance.

ACKNOWLEDGMENTS

The work is supported by a grant from the Australian Research Council. NC is the recipient of an Australian Postgraduate Award. We thank Drs. Sandy Anderson and Anna MacIntyre for the availability of the Dinkihater; Mr. Tony Romeo for assistance in SEM and freeze fracture; Dr. Andrew McLachlan and Ms Karen Smith for proofreading the manuscript and making valuable suggestions.

REFERENCES

1. E. M. Philips, M. T. Carvajal, and M. M. Munroe. Characterizing variable amorphous content in powders for inhalation. In R. N. Dalby, P. N. Byron, S. J. Farr (eds.), *Respiratory Drug Delivery V*, Interpharm Press Inc., Baffalo Grove, IL, 253–260 (1996).
2. H.-K. Chan, A. Clark, I. Gonda, M. Mumenthaler, and C. Hsu. Spray dried powders and powder blends of recombinant human deoxyribonuclease (rhDNase) for aerosol delivery. *Pharm. Res.* **14**:431–437 (1997).
3. S. D. Anderson, J. Brannan, J. Spring, N. Spalding, L. T. Rodwell, H.-K. Chan, I. Gonda, A. M. Walsh, and A. R. Clark. A new method for bronchial-provocation testing in asthmatic subjects using a dry powder of mannitol. *Am. J. Respir. Crit. Care Med.* **156**:758–765 (1997).
4. E. Daviskas, S. D. Anderson, J. D. Brannan, H.-K. Chan, S. Eberl, and G. Bautovich. Inhalation of dry-powder mannitol increases mucociliary clearance. *Eur. Respir. J.* **10**:2449–2454 (1997).
5. M. A. Braun, R. Oschmann, and P. C. Schmidt. Influence of excipients and storage humidity on the deposition of disodium cromoglycate (DSCG) in the twin impinger. *Int. J. Pharm.* **135**:53–62 (1996).
6. P. Zanen, P. I. van Spiegel, H. van der Kolk, E. Tushuizen, and R. Enthoven. The effect of the inhalation flow on the performance of a dry powder inhalation system. *Int. J. Pharm.* **81**:199–203 (1992).
7. A. H. de Boer, D. Gjaltema, and P. Hagedoorn. Inhalation characteristics and their effects on in vitro drug delivery from dry powder inhalers. Part 2: Effect of peak flow rate (PIER) and inspiration time on the in vitro drug release from three different types of commercial dry powder inhalers. *Int. J. Pharm.* **138**:45–56 (1996).
8. D. L. French, D. A. Edwards, and R. W. Niven. The influence of formulation on emission, deaggregation and deposition of dry powders for inhalation. *J. Aerosol Sci.* **27**:769–783 (1996).
9. V. A. Philip, R. C. Mehta, and P. P. Deluca. In vitro and in vivo respirable fractions of isopropanol treated PLGA microspheres using a dry powder inhaler. *Int. J. Pharm.* **151**:175–182 (1997).
10. A. R. Clark and A. M. Hollingworth. The relationship between powder inhaler resistance and peak inspiratory conditions in healthy volunteers—Implications for in vitro testing. *J. Aerosol Med* **6**:99–110 (1993).
11. D. M. Mitchell, M. A. Solomon, S. E. J. Tolfree, M. Short, and S. G. Spiro. Effect of particle size of bronchodilator aerosols on lung distribution and pulmonary function in patients with chronic asthma. *Thorax.* **42**:457–461 (1987).
12. M. M. Clay, D. Pavia, and S. W. Clarke. Effect of aerosol particle size on bronchodilation with nebulised terbutaline in asthmatic subjects. *Thorax.***41**:364–368 (1986).
13. D. Ganderton and N. M. Kassem. Dry powder inhalers. In: D. Ganderton, T. Jones (eds.), *Advances in Pharmaceutical Sciences*, Academic Press London, 1992, 165–191.
14. B. W. Low and F. M. Richards. The use of the gradient tube for the determination of crystal densities. *J. Am. Chem. Soc.* **74**:1660–66 (1952).
15. H.-K. Chan and I. Gonda. Solid state characterization of spray-dried powders of recombinant human deoxyribonuclease (RhDNase). *J. Pharm. Sci.* **87**:647–654. (1998).
16. L. Asking and B. Olsson. Calibration at different flow rates of a multistage liquid impinger. *Aerosol Sci. Tech.* **27**:39–49 (1997).
17. S. Budavari. *The Merck Index: an encyclopedia of chemicals, drugs, and biologicals*, Merck & Co. Inc., Whitehouse Station, NJ, 1996, pp. 979.
18. A. Wade and P. J. Weller. *Handbook of Pharmaceutical Excipients*. Pharmaceutical Press, London, 1994, pp. 294–298.
19. I. Gonda, Phyisco-chemical principles in aerosol delivery, In D. J. A. Crommelin and K. K. Midha (eds.), *Topics in Pharmaceutical Sciences 1991*, Medpharm Sci. Publ, Stuttgart, 1992, Ch. 7, pp. 95–115.
20. N. A. Fuchs. *The Mechanics of Aerosols*, Pergamon Press, Oxford, 1964, pp. 353–377.
21. A. D. Zimon. Adhesion of Dust and Powder, Plenum Press, New York, 1969, pp. 22–36.
22. K. J. Smith, H.-K. Chan, and K. F. Brown. Influence of flow rate on aerosol particle size distributions from pressurised and breath-actuated inhalers. *J. Aerosol Med* **11**:231–245 (1998).
23. J. Visser. Particle adhesion and removal: a review. *Particulate Sci. Technol.* **13**:169–196 (1995).
24. M. Soltani and G. Ahmadi. On particle adhesion and removal mechanisms in turbulent flows. *J. Adhesion Sci. Technol.* **8**:763–785 (1994).